

Universitat de Lleida

Document downloaded from:

<http://hdl.handle.net/10459.1/71019>

The final publication is available at:

<https://doi.org/10.1080/10589759.2010.545128>



Està subjecte a una llicència de
[Reconeixement-NoComercial-SenseObraDerivada 4.0 de Creative Commons](https://creativecommons.org/licenses/by-nc-nd/4.0/)

RESEARCH ARTICLE

An eddy-current-based sensor for preventing knots in metallic wire drawing processes

Bernat Esteban^a, Jordi-Roger Riba^{a*}, Grau Baquero^a, Cèsar Ferrater^b

^aEscola d'Enginyeria d'Igualada, Universitat Politècnica de Catalunya, 08700 Igualada, Catalunya, Spain

^bDepartament de Física Aplicada i Òptica, and Institut de Nanociència i Nanotecnologia (IN2UB), Universitat de Barcelona, 08028 Barcelona, Catalunya, Spain

*Corresponding author. Email: jordi@uetii.upc.edu.

Abstract

During metallic wire drawing processes, the presence of knots and the failure to detect them can lead to long production interruptions, significant economic losses and a lower quality of final product. Consequently, there is a pressing need to develop methods for real-time detection and prevention of this fault.

In this paper a sensor to prevent the formation of knots during the metallic wire drawing process is presented and evaluated by means of experimental data. This fast, inexpensive, non-contact sensor is based on electromagnetic principles such as eddy current induction, magnetic reluctance variations and magnetic coupling. The proposed sensor can detect knots in a target metallic wire without direct contact by measuring the impedance variations of a calibrated sensing coil caused either by a knot or an unwound loop rising from a wire rod. The incorporation of this type of sensor into a wire drawing machine can avoid the tightening of the knot, thereby reducing downtime and increasing the security and reliability of the process.

Experiments were conducted using a scale model of the above proposed system. This allowed to highlight the sensor's potential by carrying out an automatic, real-time knot detection during steel wire drawing.

Keywords: eddy currents, sensing coil, metallic wire, knots, quality control.

1. Introduction

It is well known that reduced budgets and increased market demand are leading industries to demand ever faster and more reliable manufacturing machinery. Thus, industrial companies must optimize production processes in order to reduce manufacturing time without compromising quality or compliance standards. This calls for early detection of errors [1]. Ensuring the quality of new steel products and stabilizing the quality of existing ones are important concerns for steel producers, as the mechanical properties of rod wire are being pushed to their limits [2]. This situation, coupled with the ever increasing speed of wire manufacturing, constitutes a serious challenge for real-time automatic quality control inspection systems.

Indeed, the speed of wire manufacturing is up to 3 times faster for steel wire production than in 1990. Increases in speed have caused serious problems in the first stage of wire drawing lines: the unwinding of raw material, where knots can develop due to incorrectly wound reels.

Manufacturing speeds for other materials such as copper and stainless steel have increased at a slower rate because of the distinct properties of each type of material. For example, copper is very ductile and the increase in speed is concentrated in the last steps of the drawing process. Stainless steel is a completely different case; it does not allow high speeds due to its hardness (Table 1). For wire of a diameter greater than 12mm, stretching processes are much slower, making knotting extremely uncommon, while knotting is virtually impossible when using steel bars as raw material instead of reels.

(Here Table 1)

The formation of knots in metallic wire can occur at several points in the production process, for example during reel formation, manipulation or physical unwinding. Knots can originate during reel formation as a result of misplaced turns and/or unwinding several turns at the same time [3]. Suzuki et al. [4] explain how the elastic force of a wire can generate a spring effect in some turns which can result in tangling. However, other defects, related to steel inclusions or composition, may also arise during the wire production process [5].

In this work, an eddy-current-based sensor to prevent knots forming during the metallic wire drawing process was developed and analyzed by means of experiments. The proposed sensor can detect knots formed in a target

metallic wire without direct contact. The use of this type of sensor in a wire drawing machine can avoid the tightening of the knot, thereby reducing downtime and increasing the security and reliability of the process which affects the final quality of the product.

1.1. Knot formation

A knot is formed when one or more loops from the wire rod are incorrectly unwound. When a wire drawing line operates normally, the wire loops are pulled upwards towards the tower in order to unwind them one by one. The problem occurs when a group of loops are incorrectly unwound causing them to reach the hard metal ring before the pulley. At this point the loop can potentially go through the ring and form a knot. Figures 1a and 1b show knots formed by one (a) and various (b) loops which have gone through the ring and the pulley.

When a knot is formed there are only two solutions available: cutting the wire before and after the knot or untying the knot. Depending on the size and tension of the knot, a solution is selected. The main problems caused by knots are loss of production and damage to the pay-off machine.

(Here Figure 1)

1.2. Measures for avoiding knots in wire drawing lines

To avoid knot formation, wire drawing machine manufacturers have adopted the following measures [6]:

- Increased tower height: This system increases the tower height and gives more distance for the loops to unwind. Tower height is currently 6m, but can reach up to 9m to minimize this problem. However, warehouses limit the tower height, usually with a ceiling cap of 6-7m.
- Motorized stem: This system makes the rod turn backwards to help the unwinding process. It forces a batch working procedure which prevents one rod soldering with another thereby introducing brief interruptions to the process.
- Mechanical knot detector: These are the most commonly used mechanical systems. They detect the pull of the knot once it reaches the top of the pay-off tower. In some systems this tension causes the displacement of a cam that gives an electrical signal. Other systems mechanically detect the knot before it reaches the top of the tower and generate a signal to stop the machine. The major disadvantage of these systems is that they detect the knot once it is fully formed. The operator must then completely cut

the knot and weld the wire ends.

Other systems have also been developed to reliably unwind the wire rod. For example, F. Morival and A. Morival [3] developed a gripping system for big wire reels with a vertical axis that keeps the coil stationary while the wire is unwound upwardly from the hollow of the coil.

This paper analyzes a system which detects the knot just before it forms and tightens. Thus the system has the potential to reduce production, maintenance and quality problems caused by knots. The proposed system is based on installing a coil at the top of the tower to detect unwound wire loops which could generate a knot.

Desirable features of this system for detecting knots during the wire drawing process include its robustness, the non-contact feature which avoids premature wear of mechanic parts, high sensitivity, speed and finally its flexibility to operate with a wide range of wire diameters and different conductive materials.

2. Materials and methods

2.1. Eddy current testing

Nondestructive evaluation of conductive materials is a widely applied electromagnetic measurement that employs a sensing coil for detecting conductive materials. It operates based on the principle that the eddy currents induced in the tested conductive material by the oscillating magnetic field that the sensing coil generates produce changes in the electrical impedance of this coil. These impedance changes are easily measurable. One of the main advantages of eddy current inspection is the speed at which tests can be done [7]. Moreover, eddy current sensors are much less sensitive to a number of environmental variations compared with other sensor types [8].

A low-cost and simple operation, eddy current testing has been used broadly: for detecting defects and making material thickness measurements [9], for inspecting printed circuit boards [10], for assuring quality and inspecting cracks in conductive materials [7,11-13] and for alloy sorting and monitoring of metallurgical conditions such as hardness and heat treatment in conductive objects [14-16].

Various non-destructive testing methods based on eddy currents have been developed. Some conventional eddy current inspection techniques make use of sinusoidal alternating electrical current of a selected frequency to

excite the probe, whereas other techniques, such as pulsed eddy current technique, use a step function voltage that contains a broad band of frequencies to excite the probe. As a consequence, the response to this range of multiple frequencies can be measured by applying a single step function voltage. Given that the penetration depth –as detailed in equation (1)– depends on the frequency, information from a range of depths can be obtained simultaneously. Lately, pulsed eddy current testing has been shown to hold great potential for the detection of cracks and corrosion in aging metallic structures [17]. Another recently applied technique is eddy current imaging. It is based on an eddy current probe that scans a metallic sample as it is moved all over the surface of the sample. The impedance change at each probe position is used to create the eddy current image. This image provides information about the location of defects and imperfections in the metallic sample [18].

When an alternating current flows through a coil, it generates an alternating magnetic field. If a conductive object is placed in close proximity to this coil, according to Lenz's law, circular currents are induced in this object due to the effects of the alternating magnetic field. These currents are called eddy currents. Eddy currents are affected by factors such as the amplitude and frequency of the alternating magnetic field and the electrical conductivity and magnetic permeability of the conductive object. Eddy currents induced in the conductive object generate, in turn, a magnetic field that interacts with the magnetic field generated by the sensing coil, as shown in Figure 2. This results in a change of the inductance and consequently, the impedance of such a coil. The measure of the variation in this impedance is the basis of the eddy current testing system. Any change in the conductive object that significantly alters the flow of the induced eddy currents can be detected.

(Here Figure 2)

It is very difficult for the sensing coil to operate in the low-frequency range because it works by detecting time variations of the magnetic flux. Therefore, to boost the eddy current effect, electrical supply frequencies in the range of kHz [12,14] are most effective.

When dealing with conductive objects subjected to time-varying magnetic fields, the skin effect should be considered. The skin effect is the tendency of an AC current to decay rapidly with depth within a good conductor. In other words, the current tends to flow principally on the surface of the conductor. The skin or penetration depth δ is a parameter often used to measure the strength of the skin effect and is defined as,

$$\delta = (\pi \mu_r \mu_0 \sigma f)^{-1/2} \quad (1)$$

where $\mu_0 = 4\pi \times 10^{-7}$ H/m is the magnetic permeability of free space, μ_r the relative permeability of the medium, σ its conductivity in $(\Omega \cdot \text{m})^{-1}$ and f the frequency of the electrical current in Hz. From Equation (1) it is evident that as the frequency increases, the skin effect becomes more important. Thus, according to Tsukada [14], the eddy current's density depth profile can be expressed as follows,

$$I = I_0 e^{-z/\delta} e^{-jz/\delta} \quad (2)$$

where z is the depth coordinate. Equation (2) shows that the eddy currents concentrate on the surface and decrease exponentially as depth increases, thus eddy current density is not uniform in the depth direction because of skin effects.

(Here Figure 3)

Eddy current testing can also be used to inspect both ferromagnetic and non-magnetic materials. In the case of ferromagnetic materials another effect takes place, which is related to the reluctance change in the magnetic path due to the conductive object [19] as seen in Figure 3b. Any significant change in the reluctance of the magnetic circuit alters the impedance of the sensing coil and can also be detected. The reluctance of a magnetic circuit, also known as magnetic resistance, is the opposition offered in a magnetic circuit to a magnetic flux. In the case of a uniform magnetic circuit with length l and cross-sectional area A the reluctance \mathfrak{R} can be calculated as:

$$\mathfrak{R} = \frac{l}{\mu_r \mu_0 A} \quad (3)$$

Another effect that can alter the impedance of the sensing coil arises due to the magnetic coupling between this coil and the target object. This effect takes place when the object has a loop-like shape such as a circular knot, which allows flowing induced currents. When the circular closed pre-knot and the sensing coil are placed very close to each other, the two circuits are magnetically coupled because the magnetic flux produced by one circuit links with both the circuits. This effect also alters the impedance of the sensing coil.

As explained, there are three main effects that can induce changes in the impedance of the sensing coil, namely

the eddy current effect, which is the main effect when dealing with good conductors, reluctance changes due to ferromagnetic objects and magnetic coupling due to close knots. To summarize, the superimposition of the three abovementioned effects when a volume of material greater than the wire volume moves through the sensing coil induces a change of the sensing coil inductance which can be easily measured.

2.2. Electrical model of the sensing coil

In order to optimize the behaviour of the proposed sensor, building up an equivalent electrical model of the sensing coil is of vital importance. Several electrical models have been developed. For example Tian et al. [20] take into account the mutual inductance between the sensing coil and the metallic target to derive a model of the studied arrangement for ferromagnetic and non-ferromagnetic materials. As demonstrated in the following paragraphs, feeding the sensing coil with an electrical frequency very close to its resonance frequency is desirable in order to accentuate the impedance changes of the sensing coil.

As shown in section 4, the resonance frequency of practical coils is of the order of several kHz. Thus a high-frequency equivalent circuit of the coil [21], as shown in Figure 4, should be taken into account in order to understand the dependence of the coil impedance on the electrical supply frequency.

(Here Figure 4)

From Figure 4 the equivalent impedance Z_{eq} of the sensing coil can be expressed as:

$$Z_{eq} = \frac{(R + j\omega L)(-j\frac{1}{\omega C})}{R + j\omega L - j\frac{1}{\omega C}} \quad (4)$$

After some simplifications, equation (4) can be written as:

$$Z_{eq} = \frac{R + j(\omega L - \omega R^2 C - \omega^3 L^2 C)}{\omega^2 R^2 C^2 + (\omega^2 LC - 1)^2} \quad (5)$$

where its modulus is:

$$|Z_{eq}| = \frac{\sqrt{R^2 + \omega^2 L^2}}{\sqrt{\omega^2 R^2 C^2 + (\omega^2 LC - 1)^2}} \quad (6)$$

The real and imaginary parts of equation (5) are as follows:

$$\begin{cases} \text{Real}(Z_{eq}) = \frac{R}{\omega^2 R^2 C^2 + (\omega^2 LC - 1)^2} \\ \text{Imag}(Z_{eq}) = \omega \left(\frac{L - R^2 C - \omega^2 L^2 C}{\omega^2 R^2 C^2 + (\omega^2 LC - 1)^2} \right) \end{cases} \quad (7)$$

The imaginary part of equation (7) divided by the angular frequency ω is often associated to an equivalent inductance of the whole circuit shown in Figure 4b.

From equation (7), the resonance frequency ω_r can be obtained as in equation (8).

$$\omega_r = \sqrt{\frac{L - R^2 C}{L^2 C}} \quad (8)$$

Figure 5a shows the theoretical frequency dependency of the modulus of the coil impedance as explains equation (6), where the resonance frequency of the parallel circuit can be clearly appreciated in Figure 4b. From Figure 5a it can be deduced that in close proximity to the resonance frequency, the impedance changes are maximal. Thus, it is best to work near the resonance frequency in order to optimize the response of the sensor for detecting wire knots.

Figure 5b plots the $\text{Imag}(Z_{eq})/\omega$ against the frequency, obtaining an effective or equivalent inductance or capacitance, depending on whether its value is positive or negative, respectively.

(Here Figure 5)

As shown in Figure 5b, when the electrical supply frequency is higher than the resonance frequency, the circuit has a capacitive behaviour because the imaginary part of the impedance is negative. Conversely, for frequencies lower than the resonance frequency it has an inductive behaviour. As illustrated in Figure 5a, the imaginary part of the impedance experiences a sharper change in the vicinity of the resonance frequency.

3. Experimental Arrangement

The experiments were carried out using an experimental arrangement as shown in Figure 6. It consists of a sensing coil and a movable target wire containing a knot. The whole system was built at a reduced scale (1:12) compared to that of an average pay-off machine.

A 4192A Hewlett Packard impedance analyzer was used to measure the impedance of the coil and its real and imaginary parts. It enables a 5 Hz to 13 MHz variable measuring frequency.

(Here Figure 6)

Figure 7 shows a diagram of an industrial pay-off machine that incorporates the sensing system for detecting knots proposed in this work. Commercial wire rods have an average diameter of 1.2 m for steel and stainless steel wire. To avoid damage to the sensing coil a security margin is necessary; therefore, the sensing coil proposed has a 1.6 m diameter. This is the ratio between the wire rod and the sensing coil diameters that was used in the experimental arrangement.

The distance between the detection zone and the top of the pay-off machine (see Figure 7) allows the process to be stopped before the knot is completely formed. Avoiding tightening of the knot reduces downtime and increases the security and reliability of the process.

(Here Figure 7)

4. Experimental Results

The first step in checking the behaviour of the proposed wire knots sensor system, consists in calibrating the sensing coil and calculating its resonance frequency, as detailed in Figure 8. The numerical fit results in $R = 0.5 \Omega$, $L = 1.2 \text{ mH}$, $C = 2.49 \text{ pF}$ with a resonance frequency of 95.3 kHz.

(Here Figure 8)

Results from Figure 8 prove that the experimental data can be tightly adjusted by equations 6 and 7, corroborating the assumptions made in Section 2.2. Figure 8a demonstrates that the impedance of the sensing coil greatly depends on the electrical frequency, being maximized at the resonance frequency, which is close to 95 kHz for the analyzed system. Figure 8b plots the imaginary part of Z/ω for both experimental data and its

numerical fit performed by applying equation 7. The imaginary part of Z/ω is associated to the equivalent inductance of the whole circuit. This figure again corroborates the accuracy of the proposed electrical model.

In order to check the performance of the proposed system, the impedance of the sensing coil is measured when a steel wire containing a knot moves towards the sensing coil, as shown in Figure 9.

(Here Figure 9)

The experimental results shown in Figure 9 confirm that the proposed system detects the presence of a pre-knot on a steel wire moving through the sensing coil. As displayed in Figure 9, when the pre-knot gets close to the sensing coil, the modulus of $\text{Imag}(Z_{eq})/\omega$ increases, whereas when it moves away from the coil it decreases. Consequently, when a pre-knot is very close to the sensing coil it causes a sharp change in the imaginary part of the impedance, this change being easily detectable. This experiment validates the claim that the system presented in this work allows a steel wire pre-knot to be detected while moving upwards towards the top pulley of the pay-off machine.

The proposed sensor method has also been checked with non-ferromagnetic and low ferromagnetic materials: copper and stainless steel, respectively. Figure 10 shows $\text{Imag}(Z_{eq})/\omega$ when these types of metallic wires contain a pre-knot which moves towards the sensing coil.

(Here Figure 10)

Figure 10 corroborates that when dealing with wires containing a pre-knot which are made of either non-ferromagnetic materials, such as copper, or low ferromagnetic materials, such as stainless steel, a sharp change in the imaginary part of the impedance is induced when the pre-knot is very close to the sensing coil. This change is easily detectable.

The experimental results show that the proposed sensor system is more sensitive when dealing with steel and copper wires than when dealing with stainless steel wires. On the one hand, steel is a ferromagnetic material –its relative magnetic permeability μ_r is superior to 1– and has an electrical conductivity approximately four times greater than stainless steel. On the other hand, although copper is a non-ferromagnetic material with a relative magnetic permeability of $\mu_r = 1$, it has an electrical conductivity one order of magnitude higher than steel. In our

results, two main effects are explained. The first is that eddy currents are more intensely induced in materials with superior electrical conductivity. Second, the reluctance change in the magnetic path is more pronounced when ferromagnetic materials are present. Non-ferromagnetic materials such as copper do not produce changes in the magnetic reluctance of the whole circuit. The experimental results corroborate these effects, which are summarized in Table 2.

(Here Table 2)

5. Conclusions

In this paper a sensor for preventing knots during the steel wire making process was presented and then evaluated using experimental data. This sensor is based on electromagnetic principles such as eddy current induction, magnetic reluctance variations and magnetic coupling. The proposed sensor can detect changes in the thickness of a target metallic wire without direct contact.

The sensor consists of a sensing coil, the impedance of which experiences a sharp change when it detects a knot in the metallic wire moving along its perpendicular axis. Experimental results also show that the sensitivity of the system greatly improves when dealing with frequencies close to the resonance frequency of the sensing coil. In addition, the results show that the proposed sensor can effectively detect knots when dealing with both ferromagnetic and non-ferromagnetic conductive materials.

Attributes such as its speed, simplicity, low cost, and the fact that it is non-contact make this technique a viable candidate for real-time inspection of different metallic wires during manufacturing. Experiments performed using a scale model of the whole system show excellent performance results, which highlight the capability of this type of system to carry out an automated detection of knots during industrial wire making processes.

Further work carried out by the authors of this paper includes the design, implementation and evaluation of the electronic circuit necessary for automated detection of this kind of fault in the drawing process.

Acknowledgement

The authors would like to acknowledge Ramon Freixes (EXELFIL S.A.) for providing test samples and José

Cornet (MFL GROUP) for his expertise in drawing process technology.

6. References

- [1] R. Specogna, F. Trevisan, Advanced geometric formulations for the design of a long defects detection system, *Nondestruct. Test. Eval.* 24 (2009), pp. 195-207.
- [2] Y. Wan-Hua, C. Shao-Hui, K. Yong-Hai, C. Kai-Chao, Development and application of online Stelmor Controlled Cooling System, *Applied Thermal Engineering*. 29 (2009), pp. 2949-2953.
- [3] F. Morival, A. Morival, 1985. US Patent # 4,512,533.
- [4] H. Suzuki, I. Makoto, T. Atutosi, A. Yasuo, S. Yosikazu, Y. Kazuhide, 1981. US # 4,261,191.
- [5] M. Yilmaz, Failures during the production and usage of steel wires, *Journal of Materials Processing Technology*. 171 (2006), pp. 232-239.
- [6] J. Cornet, Commercial offers historical data (1990–2008 period). MFL Group®. 2008.
- [7] A. Zaoui, H. Menana, M. Feliachi, M. Abdellah, Generalization of the ideal crack model for an arrayed eddy current sensor, *IEEE Transactions on Magnetics*. 44 (2008), pp.
- [8] M. R. Nabavi, S. Nihtianov, A Novel Interface for Eddy Current Displacement Sensors, *IEEE Transactions on Instrumentation and Measurement*. 58 (2009), pp. 1623-1632.
- [9] Y. S. Cho, S. U. Hong, M. S. Lee, The assessment of the compressive strength and thickness of concrete structures using nondestructive testing and an artificial neural network, *Nondestruct. Test. Eval.* 24 (2009), pp. 277-288.
- [10] D. Kacprzak, T. Taniguchi, K. Nakamura, S. Yamada, M. Iwahara, Novel eddy current testing sensor for the inspection of printed circuit boards, *IEEE Transactions on Magnetics*. 37 (2001), pp. 2010-2012.
- [11] L. Bettaieb, H. Kokabi, M. Poloujadoff, A. Sentz, C. Tcharkhtchi, Fatigue and/or crack detection in NDE, *Nondestruct. Test. Eval.* 25 (2010) pp. 13-24.
- [12] N. Yusa, Development of computational inversion techniques to size cracks from eddy current signals, *Nondestruct. Test. Eval.* 24 (2009), pp. 39-52.
- [13] R. Hohmann, D. Lomparski, H. J. Krause, M. Von Kreurzbruck, W. Becker, Aircraft wheel testing with remote eddy current technique using a HTS SQUID magnetometer, *IEEE Transactions on Applied Superconductivity*. 11 (2001), pp. 1279-1282.
- [14] K. Tsukada, T. Kiwa, T. Kawata, Y. Ishihara, Low-frequency eddy current imaging using MR sensor detecting tangential magnetic field components for nondestructive evaluation, *IEEE Transactions on Magnetics*. 42 (2006), pp. 3315-3317.
- [15] M. Cacciola, S. Calcagno, G. Megali, F. C. Morabito, D. Pellicano, M. Versaci, FEA Design and Misfit Minimization for In-Depth Flaw Characterization in Metallic Plates With Eddy Current Nondestructive Testing, *IEEE Transactions on Magnetics*. 45 (2009), pp. 1506-1509.
- [16] W. L. Yin, P. J. Withers, U. Sharma, A. J. Peyton, Noncontact Characterization of Carbon-Fiber-Reinforced Plastics Using Multifrequency Eddy Current Sensors, *IEEE Transactions on Instrumentation and Measurement*. 58 (2009), pp. 738-743.
- [17] D. Zhou, G. Y. Tian, Y. Li, Simulation based on optimisation of pulsed eddy current probe design, *Nondestruct. Test. Eval.* Available online 04 January 2010.

- [18] H. Carreon, Detection of creep damage in a nickel-based superalloy turbine bucket using eddy current imaging, *Nondestruct. Test. Eval.* 24 (2009), pp. 233-241.
- [19] H. N. Norton, 1989. *Handbook of transducers*, Prentice-Hall, Inc. Englewood Cliffs, New Jersey.
- [20] G. Y. Tian, Z. X. Zhao, R. W. Baines, The research of inhomogeneity in eddy current sensors, *Sensors and Actuators A*. 69 (1998), pp. 148-151.
- [21] Q. Yu, T. W. Holmes, K. Naishadham, RF equivalent circuit modeling of ferrite-core inductors and characterization of core materials, *IEEE Trans. Electromagn. Compat.* 44 (2002), pp. 258-262.

TABLES

Table 1

Velocity variation of drawing machines for steel and copper (1990 to 2007) extracted from Cornet (2008).

Drawing Machine Output Diameter	1990		2007	
	Machine input	Machine output	Machine input	Machine output
	[m/s]	[m/s]	[m/s]	[m/s]
0.5 - 2 mm (Low and high carbon steel)	2 - 3 m/s	8 m/s	7-9 m/s	30-50 m/s
2 - 5 mm (Low and high carbon steel)	2 m/s	5 m/s	5-6 m/s	15-25 m/s
5 - 12 mm (Low and high carbon steel)	1 m/s	3 m/s	3 m/s	10 m/s
2 -3 mm (Copper)	1 m/s	20-25 m/s	1.5 m/s	30-35 m/s
2-4 mm (Stainless steel)	0.5-1 m/s	2-5 m/s	1-2 m/s	3-6 m/s

Table 2

Effects related to material properties which contribute to the pre-knot detection.

Material properties	Electrical conductivity	Magnetic permeability
Physical effects	Induced eddy currents	Reluctance changes
Steel	Medium	High
Stainless steel	Low	Low
Copper	Very high	Null

FIGURES

Figure 1. Knots formed during drawing process.

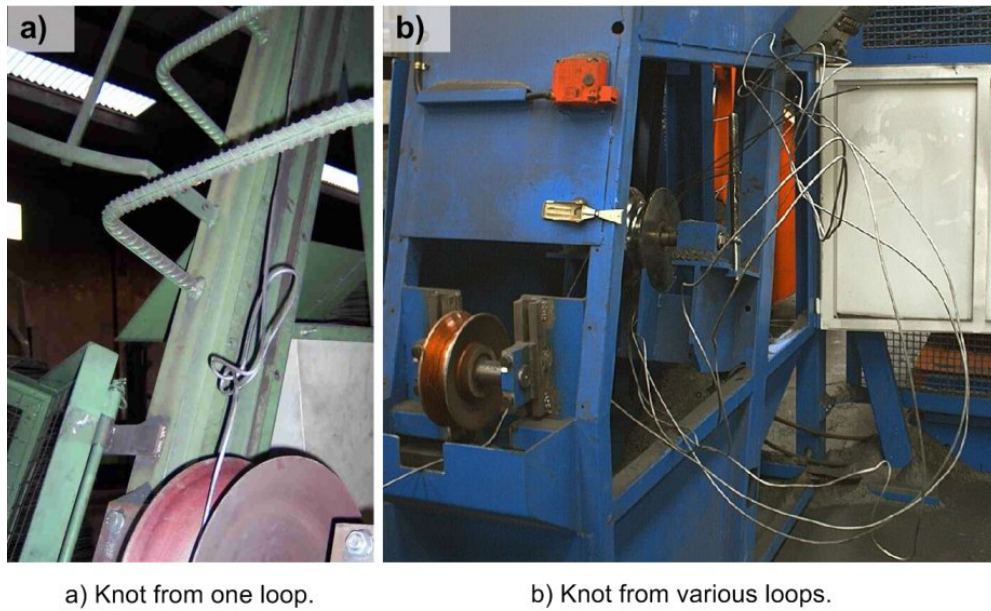


Figure 2. Currents induced in a conductive object with both ends electrically insulated. Figure 2a shows the eddy currents induced in a straight wire rod. Figure 2b shows the current induced in a wire rod with a closed pre-knot.

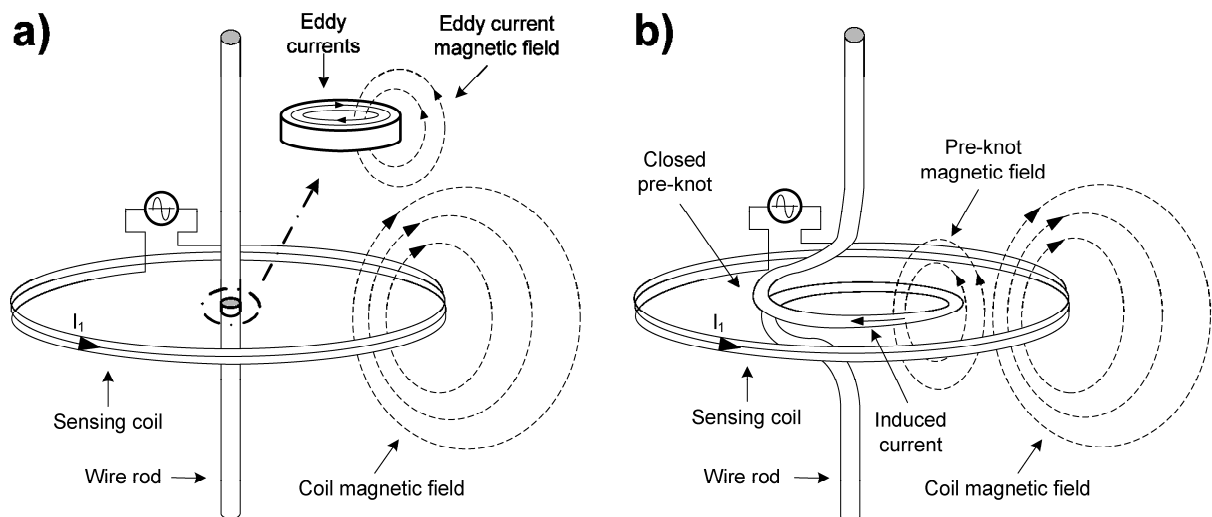


Figure 3. Finite elements simulation of the magnetic field generated by a coil. Changes in the magnetic flux path due to material conductivity.

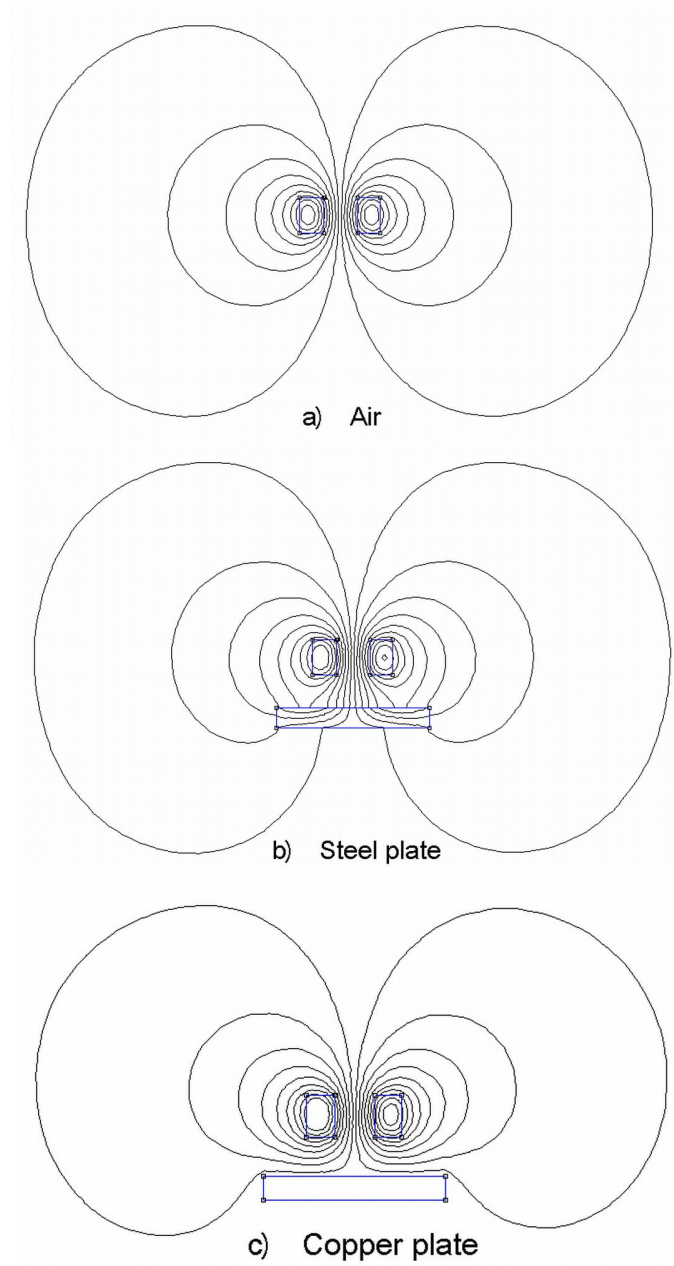


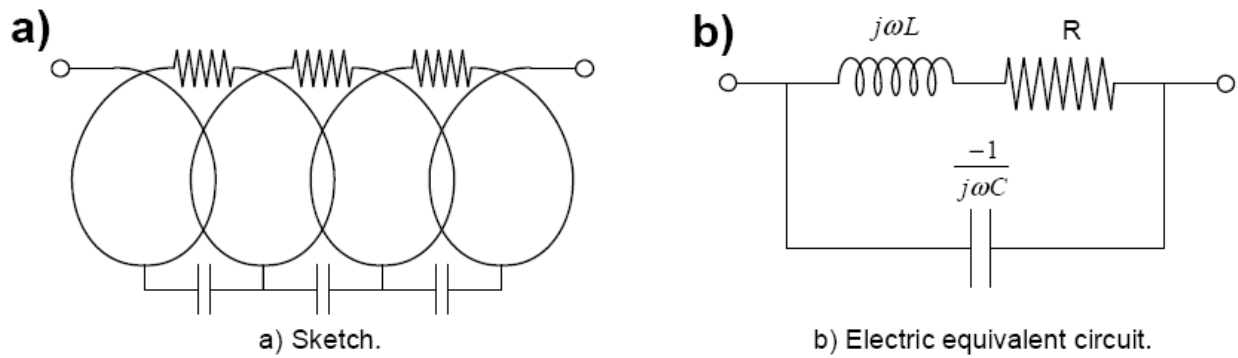
Figure 4. High-frequency equivalent circuit of a coil.

Figure 5. Frequency dependency of the modulus and effective inductance of the circuit shown in **Fig. 4b.** as a function of the electrical supply frequency, when $R=1\ \Omega$, $L=0.2\ \text{mH}$ and $C=12.7\ \text{nF}$. Using these values, the resonance frequency is 100 kHz.

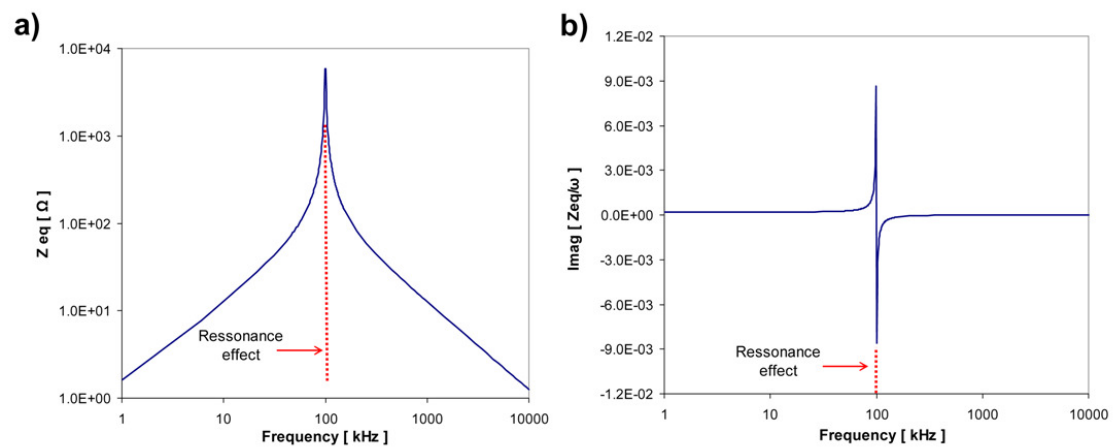


Figure 6. Experimental layout for detecting the knot developed in the sliding conductive wire which moves through the sensing coil.

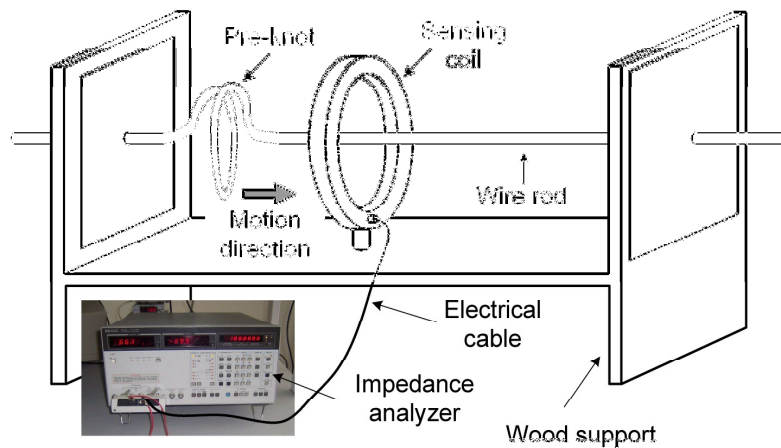


Figure 7. Diagram of the proposed sensor system including the wire rod and the sensing coil.

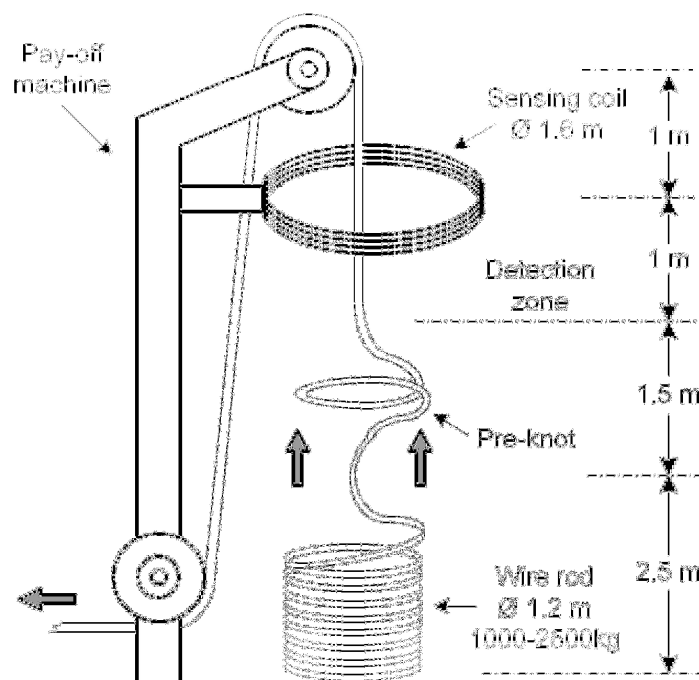


Figure 8. Experimental values and numerical fit. a) Frequency dependency of the modulus of the equivalent impedance of the coil. b) Frequency dependency of $\text{Imag}(Z_{eq})/\omega$.

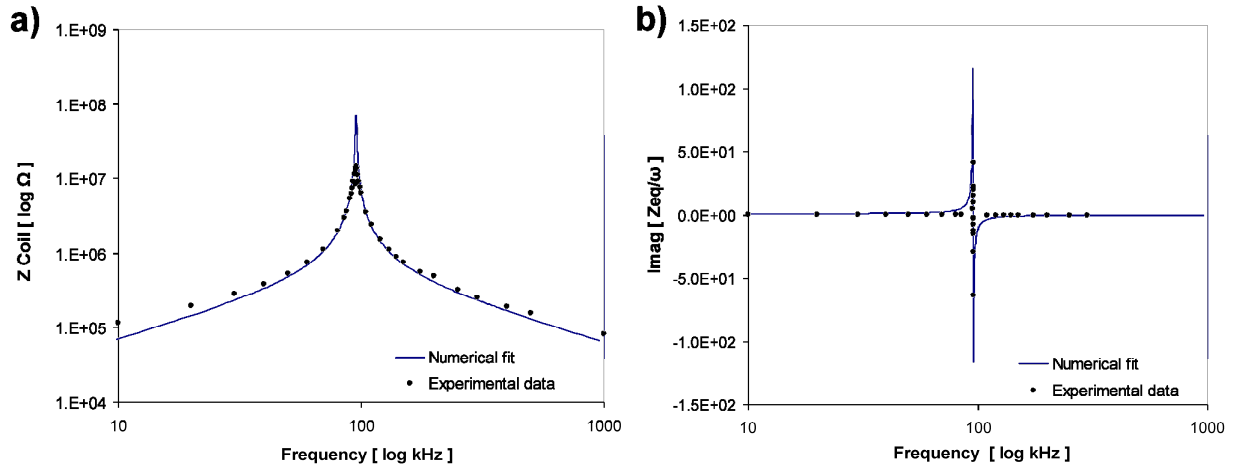


Figure 9. $\text{Imag}(Z_{eq})/\omega$ of the sensing coil against distance between the centres of the steel wire pre-knot and the sensing coil.

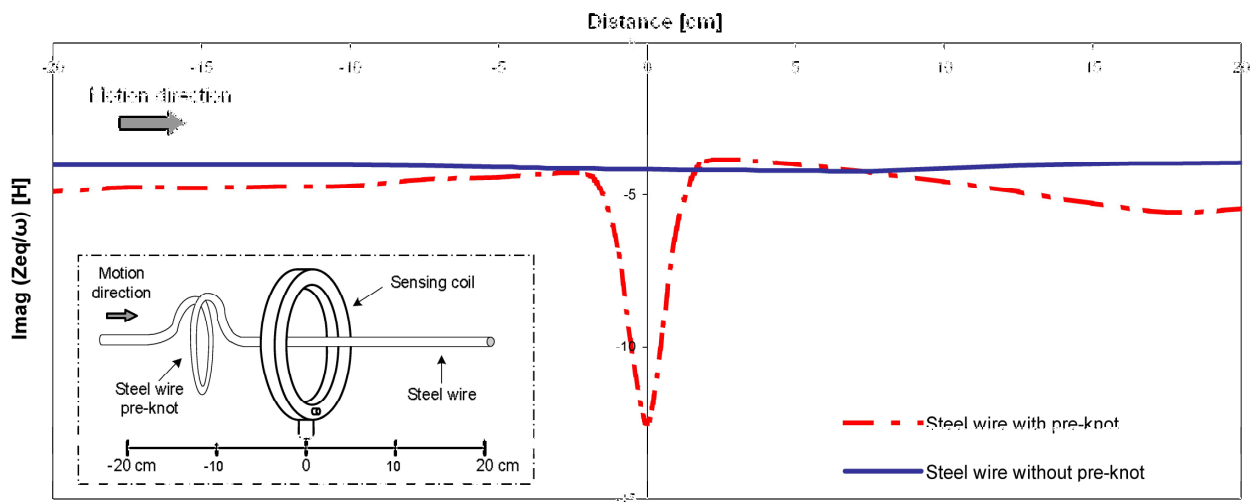


Figure 10. $\text{Imag}(Z_{\text{eq}})/\omega$ of the sensing coil against distance between the centres of the copper or stainless steel wire pre-knot and the sensing coil.

